

RESEARCH ARTICLE

# Development of a low-distortion authalic sphere for the oblique azimuthal equal-area map projection of the spheroid

Kerkovits Krisztián

Institute of Cartography and Geoinformatics, ELTE Eötvös Loránd University, Budapest, Hungary

*Received: September 27, 2024; returned: March 10, 2025; revised: May 29, 2025; accepted: May 29, 2025.*

---

**Abstract:** This paper gives a new possible realization of the oblique Lambert Azimuthal Equal-Area map projection for the ellipsoid of revolution. Unlike the realization available in previous literature, the authalic sphere used for the derivation has very low distortion at the neighborhood of a freely chosen standard parallel. For this reason, the distortions caused by this authalic sphere can be neglected. It is shown that this realization gives a better approximation of the azimuthal equal-area mapping of the sphere in terms of angular distortions. Interesting side results of the study include a numerically stable inverse formulation for the azimuthal equal-area map of the sphere and mathematical connections between the Gaussian conformal sphere and the low-distortion authalic sphere.

**Keywords:** Lambert Azimuthal Equal-Area, auxiliary spheres, oblique map projections, authalic sphere, double mapping

---

## 1 The purpose of this study

Thematic maps usually require equal-area mappings. Several methods of cartographic visualization can be misleading if not applied on an equivalent map projection [6]. Especially statistical data are very sensitive to areal distortions.

To fulfil this need, plenty of equal-area map projections have been developed [10]. One of the most popular equivalent mappings for regional maps is the Lambert Azimuthal Equal-Area (hereafter LAEA) projection. It is usually recommended for circular areas [9].

If the center of the area is not at one of the poles, we should use it in the oblique aspect. A notable example is the coordinate system LAEA-EU registered as EPSG:3035 [3].

Oblique map projections of the sphere are created by rotating the graticule and placing a metapole (or pseudopole) onto the center of the area [7, 14]. However, the accuracy of the terrestrial sphere is insufficient for medium-scale maps. The ellipsoid of revolution does not have the same degree of symmetry as the sphere, it is impossible to rotate the graticule on its surface. Thus, oblique map projections of the ellipsoid need special care. We should note that while the oblique aspect of a spherical mapping is always unique, this is not the case for the ellipsoid of revolution [14]. For example, the oblique stereographic map of the ellipsoid has three different known realizations: the double stereographic [13], the Roussilhe stereographic [8], and the Thomas stereographic [10], not to mention the possibility to invent new ones.

As far as the author is concerned, only Reference [10] have listed a possible formulation for an oblique LAEA of the ellipsoid. He developed that as a double mapping through an authalic sphere. However, that formulation has two drawbacks. First, the authalic sphere used by Snyder has some angular distortions at the origin. He corrected for it by an affine transform on the final map, but even Snyder admitted that with this step the resulting map is slightly non-azimuthal. We will see that this non-azimuthality influences the angular distortion pattern of the map. Second, the inverse formulae given by Snyder are unnecessarily complicated even for the spherical variant. Furthermore, neither Snyder nor any later study have listed formulae for the distortions of the ellipsoidal LAEA, so every distortion analysis apparently used spherical formulae.

This paper has three major achievements over previous literature:

1. A simpler and more robust formulation is given for the inverse oblique LAEA projection, which can be used as a drop-in replacement for Snyder's formulae.
2. A new low-distortion authalic sphere is developed based on the idea of Gauß [2].
3. It lists analytical formulae for the distortions of the ellipsoidal oblique LAEA.

## 2 Oblique azimuthal equal-area projection of the sphere

Reference [10] lists the direct and inverse formulae of the oblique LAEA of the sphere. The inverse formulae are, however, unnecessarily complicated, successively apply trigonometric and inverse trigonometric functions. As this may waste computing resources and introduces numerical instability near the origin of the coordinate system, a simpler form of the inverse is developed here. To develop this formulation, intermediate steps are used from the derivation of direct formulae. Therefore, the derivation of the direct formulae in Reference [10] is repeated here.

Let us introduce the following polar coordinate system:

$$x = \varrho \sin \lambda' \quad (1)$$

$$y = -\varrho \cos \lambda' \quad (2)$$

Here  $\varrho(\varphi')$  is the radius of metalatitude  $\varphi'$ , and polar angle  $\lambda'$  is the metalongitude. Metalatitude and metalongitude (also known as pseudolatitude and pseudolongitude) are identical to latitude and longitude in the normal aspect, and are calculated using a spatial rotation if the aspect of the map projection is oblique [7]:

$$\sin \varphi' = \sin \varphi \sin \varphi_0 + \cos \varphi \cos \varphi_0 \cos(\lambda - \lambda_0) \quad (3)$$



$$\cos \varphi' \sin \lambda' = \cos \varphi \sin(\lambda - \lambda_0) \quad (4)$$

$$\cos \varphi' \cos \lambda' = -\sin \varphi \cos \varphi_0 + \cos \varphi \sin \varphi_0 \cos(\lambda - \lambda_0) \quad (5)$$

The formulation above defines a coordinate system on the sphere with the metapole located at geographic coordinates  $\varphi_0, \lambda_0$ , and its prime metameridian points to South. The direction of the prime metameridian is insignificant in the context of this study, as it only rotates the resulting map on the plane.

If we are on a sphere of radius  $R$ , then the formula of the LAEA in normal aspect is [10]:

$$\varrho = 2R \sin\left(\frac{\pi}{4} - \frac{\varphi'}{2}\right) = \sqrt{2}R \sqrt{2 \sin^2\left(\frac{\pi}{4} - \frac{\varphi'}{2}\right)} = \sqrt{2}R \sqrt{1 - \cos\left(\frac{\pi}{2} - \varphi'\right)} \quad (6)$$

Thus, we will use later:

$$\varrho = \sqrt{2}R \sqrt{1 - \sin \varphi'} \quad (7)$$

Multiplying and dividing by  $\sqrt{1 + \sin \varphi'}$ :

$$\varrho = \sqrt{2}R \frac{\cos \varphi'}{\sqrt{1 + \sin \varphi'}} \quad (8)$$

Substituting this into (1) and (2):

$$x = \sqrt{2}R \frac{\cos \varphi' \sin \lambda'}{\sqrt{1 + \sin \varphi'}} \quad (9)$$

$$y = \sqrt{2}R \frac{-\cos \varphi' \cos \lambda'}{\sqrt{1 + \sin \varphi'}} \quad (10)$$

Applying formulae (3) to (5):

$$x = \sqrt{2}R \frac{\cos \varphi \sin(\lambda - \lambda_0)}{\sqrt{1 + \sin \varphi \sin \varphi_0 + \cos \varphi \cos \varphi_0 \cos(\lambda - \lambda_0)}} \quad (11)$$

$$y = \sqrt{2}R \frac{\sin \varphi \cos \varphi_0 - \cos \varphi \sin \varphi_0 \cos(\lambda - \lambda_0)}{\sqrt{1 + \sin \varphi \sin \varphi_0 + \cos \varphi \cos \varphi_0 \cos(\lambda - \lambda_0)}} \quad (12)$$

To develop the inverse, we should first note from equations (1), (2), and (7) that:

$$x^2 + y^2 = \varrho^2 = 2R^2(1 - \sin \varphi') \quad (13)$$

Let us introduce the auxiliary variable  $t$ :

$$t = \frac{x^2 + y^2}{2R^2} \quad (14)$$

From (13):

$$\sin \varphi' = 1 - t \quad (15)$$

Using (3) and rearranging:

$$\cos \varphi \cos(\lambda - \lambda_0) = \frac{1 - t - \sin \varphi \sin \varphi_0}{\cos \varphi_0} \quad (16)$$

Substituting the two previous equations into (12):

$$y = \sqrt{2}R \frac{\sin \varphi \cos \varphi_0 - \sin \varphi_0 \frac{1-t-\sin \varphi \sin \varphi_0}{\cos \varphi_0}}{\sqrt{2-t}} = \sqrt{2}R \frac{\sin \varphi - (1-t) \sin \varphi_0}{\sqrt{2-t} \cos \varphi_0} \quad (17)$$

This is easily solved for  $\varphi$ :

$$\varphi = \arcsin \left[ \frac{y \sqrt{2-t} \cos \varphi_0}{\sqrt{2}R} + (1-t) \sin \varphi_0 \right] \quad (18)$$

Note that apart from the trigonometric functions of  $\varphi_0$  (which has to be computed only once for a specific mapping), only one trigonometric function is needed to solve  $\varphi$  for each point. Reference [10] needed 3 trigonometric functions for each point. We should also note that there is now no division by  $\varphi$ , which resolves the numerical instability of Snyder's equations close to the origin.

We can do the same substitution into (11) (note that  $\sin \lambda = \tan \lambda \cos \lambda$ ):

$$x = \sqrt{2}R \frac{\tan(\lambda - \lambda_0) \frac{1-t-\sin \varphi \sin \varphi_0}{\cos \varphi_0}}{\sqrt{2-t}} \quad (19)$$

Using solution (18) for  $\varphi$ :

$$\begin{aligned} x &= \sqrt{2}R \frac{\tan(\lambda - \lambda_0) \left( 1-t - \left[ \frac{y \sqrt{2-t} \cos \varphi_0}{\sqrt{2}R} + (1-t) \sin \varphi_0 \right] \sin \varphi_0 \right)}{\cos \varphi_0 \sqrt{2-t}} \\ &= \frac{\tan(\lambda - \lambda_0) \left[ \sqrt{2}R(1-t) \cos \varphi_0 - y \sqrt{2-t} \sin \varphi_0 \right]}{\sqrt{2-t}} \end{aligned} \quad (20)$$

Solving for  $\lambda$ :

$$\lambda = \lambda_0 + \arctan \frac{x \sqrt{2-t}}{\sqrt{2}R(1-t) \cos \varphi_0 - y \sqrt{2-t} \sin \varphi_0} \quad (21)$$

Again, the number of trigonometric functions needed for each point is reduced from three to one compared to Snyder's formulation. The formulae of Reference [10] would result in division 0/0 near the origin, the formulae listed here do not have this problem. Please note that function arctan should be implemented using function atan2 in common programming languages.

The inverse formulation listed here should always be possible to evaluate, theoretically no square roots of negative numbers and no division by zero (assuming the application of function atan2) is possible in the domain of the full map ( $0 \leq t \leq 2$ ). However, due to floating-point errors,  $t$  might be slightly greater than 2. In this case,  $\varphi = -\varphi_0$  and  $\lambda = \lambda_0 \pm \pi$ . Equation (21) is numerically unstable close to  $\varphi = \pm \pi/2$  (as through  $x = 0$ ,  $1-t = \pm \sin \varphi_0$ , and  $y = \pm \sqrt{2}R \cos \varphi_0 / \sqrt{2-t}$ , this results in 0/0), but in this case, longitude is not defined anyway.



### 3 General authalic sphere

To develop a map projection in transverse or oblique aspect, the most convenient possibility is to use a metageographic (pseudogeographic) coordinate system [14], just as we have done it previously. However, an ellipsoid of revolution does not have a full rotational symmetry as the sphere: its graticule cannot be rotated on its surface. It is possible to construct oblique ellipsoidal map projections by generalizing the properties of spherical map projections, a good example for this method is given by Reference [4] for an ellipsoidal gnomonic projection. This has the advantage that the distortion characteristics of the resulting map will exactly follow our expectations. However, the design of such map projections is usually not straightforward.

A popular alternative is to use a double mapping, that is, we first map the ellipsoid onto an auxiliary sphere and use the oblique map projection from the sphere to the plane. The advantage of this method is that it is easy to develop. However, it is impossible to map the ellipsoid of revolution onto a sphere without distortion. These distortions will influence the distortion pattern of the resulting map projections. To answer this problem, multiple auxiliary spheres were created [1], a conformal one for conformal maps, an authalic one for equal-area maps, and a rectifying one for equidistant maps. We should note that the rectifying sphere is equidistant only along meridians, which already shows a limitation of this approach.

These auxiliary spheres were created for a global scale: the Equator is mapped to the Equator, poles are mapped to the poles on the sphere. This usually also restricts the radius of the auxiliary sphere and the linear distortions cannot be adjusted. Gauß was the first to create an auxiliary (conformal) sphere for regional use [2]. He demonstrated that the local distortions of auxiliary spheres can be significantly reduced around a freely chosen parallel, if we relax the condition that the full surface of the ellipsoid must be mapped exactly to the full surface of the sphere. Such a low-distortion conformal sphere is used now for, among others, the official map projections of the Netherlands, Switzerland, Czechia, and Hungary, which demonstrate the usefulness of this approach. However, no low-distortion authalic sphere has been developed yet.

To avoid confusion, uppercase Greek letters  $\Phi, \Lambda$  will denote geographic coordinates on the ellipsoid and their lowercase versions  $\varphi, \lambda$  are used on the authalic sphere.  $a$  and  $b$  stand for the major and minor semi-axes of the ellipsoid.  $N(\Phi)$  is the prime-vertical radius of curvature,  $M(\Phi)$  is the meridional radius of curvature,  $c$  is the polar radius of curvature, first and second eccentricity is denoted by  $e$  and  $e'$ :

$$e = \sqrt{\frac{a^2 - b^2}{a^2}} \quad (22)$$

$$e' = \sqrt{\frac{a^2 - b^2}{b^2}} = \frac{e}{\sqrt{1 - e^2}} \quad (23)$$

$$c = N(90^\circ) = M(90^\circ) = \frac{a}{\sqrt{1 - e^2}} \quad (24)$$

$$v(\Phi) = \frac{\sqrt{1 - e^2 \sin^2 \Phi}}{\sqrt{1 - e^2}} = \sqrt{1 + (e')^2 \cos^2 \Phi} \quad (25)$$

$$\frac{dv}{d\Phi} = \frac{-2(e')^2 \cos \Phi \sin \Phi}{2\sqrt{1 + (e')^2 \cos^2 \Phi}} = \tan \Phi \frac{1 - v^2(\Phi)}{v(\Phi)} \quad (26)$$

$$N(\Phi) = \frac{a}{\sqrt{1 - e^2 \sin^2 \Phi}} = \frac{c}{v(\Phi)} \quad (27)$$

$$M(\Phi) = \frac{a(1 - e^2)}{(1 - e^2 \sin^2 \Phi)^{3/2}} = \frac{c}{v^3(\Phi)} \quad (28)$$

We will assume that parallels are mapped to parallels, and meridians to meridians on the sphere. Therefore, lunes of the ellipsoid must be mapped to lunes on the sphere. Their area must be equal to each other (the sphere must be authalic) and the area of the lune is a linear function of the longitude difference both on the sphere and on the ellipsoid of revolution. Therefore:

$$\lambda = n(\Lambda - \Lambda_0) \quad (29)$$

Here,  $n > 0$  and  $\Lambda_0$  allows changing the Prime Meridian on the authalic sphere. It is recommended that  $\Lambda_0$  is the longitude of the origin so that we can use  $\Lambda_0 = 0$  on the sphere.

We will next calculate the linear scales  $h$  and  $k$  along meridians and parallels as the ratio between infinitesimal lengths on the sphere of radius  $R$  and the ellipsoid:

$$h = \lim_{\Delta\Phi \rightarrow 0} \frac{R \Delta\varphi}{M(\Phi) \Delta\Phi} = \frac{R}{M(\Phi)} \frac{d\varphi}{d\Phi} \quad (30)$$

$$k = \lim_{\Delta\Lambda \rightarrow 0} \frac{R \cos \varphi \Delta\lambda}{N(\Phi) \cos \Phi \Delta\Lambda} = \frac{Rn \cos \varphi}{N(\Phi) \cos \Phi} \quad (31)$$

Above, we used from (29) that the derivative of  $\lambda$  with respect of  $\Lambda$  is  $n$ . Because meridians and parallels are perpendicular both on the ellipsoid and the sphere, they are principal directions [11]. Therefore, the sphere is authalic if  $hk = 1$ , that is:

$$\frac{d\varphi}{d\Phi} = \frac{M(\Phi) N(\Phi) \cos \Phi}{R^2 n \cos \varphi} \quad (32)$$

Separating variables, integrating it and taking the arcsine of both sides:

$$\varphi = \arcsin \left[ \frac{a^2(1 - e^2)}{R^2 n} \left( \frac{1}{2} \cdot \frac{\sin \Phi}{1 - e^2 \sin^2 \Phi} + \frac{1}{4e} \ln \frac{1 + e \sin \Phi}{1 - e \sin \Phi} \right) + \kappa \right] \quad (33)$$

$\kappa$  is a constant of integration. Note that we get the usual authalic sphere by choosing  $\kappa = 0$ ,  $n = 1$ , and  $R$  equal to the authalic radius. To get the inverse formula, (29) is solved easily for  $\Lambda$ :

$$\Lambda = \frac{\lambda}{n} + \Lambda_0 \quad (34)$$

(33) cannot be inverted analytically. First, we transform the equation to:

$$\frac{(\sin \varphi - \kappa) R^2 n}{a^2(1 - e^2)} - \frac{1}{2} \cdot \frac{\sin \Phi}{1 - e^2 \sin^2 \Phi} - \frac{1}{4e} \ln \frac{1 + e \sin \Phi}{1 - e \sin \Phi} = 0 \quad (35)$$

$\Phi$  can now be solved by the Newton–Raphson formula:

$$\Phi = \Phi + \frac{1 - e^2 \sin^2 \Phi}{\cos \Phi} \left[ \frac{(\sin \varphi - \kappa) R^2 n}{a^2 (1 - e^2)} - \frac{1}{2} \cdot \frac{\sin \Phi}{1 - e^2 \sin^2 \Phi} - \frac{1}{4e} \ln \frac{1 + e \sin \Phi}{1 - e \sin \Phi} \right] \quad (36)$$

Where substitute an initial guess for  $\Phi$  into the right-hand side to get a better estimate and repeat the calculation until the correction is sufficiently small. Discussion on the initial guess and convergence is given later. Please note that a series representation of the inverse like it was done by Reference [1] is not possible: parameters  $R$ ,  $n$ , and  $\kappa$  varies with the area of interest.

## 4 Parameters for a low-distortion authalic sphere

We have yet to determine the parameters  $n$  and  $\kappa$ . Furthermore, as we relaxed the condition that the full ellipsoid is mapped to the full sphere,  $R$  is not the authalic radius, but it can be adapted to our region of interest. Following Reference [2], we shall pick an arbitrary latitude  $\Phi_0$ . This will be a standard parallel of our auxiliary sphere ( $h = k = 1$ ). In addition, we expect that the first two derivatives of linear scales  $h$  and  $k$  with respect to  $\Phi$  vanish at  $\Phi_0$ , that is, the distortions in the small neighborhood of  $\Phi_0$  are effectively zero. This will make our authalic sphere almost distortion-free locally, so the distortions of the double mapping will almost solely be controlled by the sphere-to-plane mapping.

As  $h = 1/k$ , if the derivatives of  $k$  vanish at a point then the derivatives of  $h$  must also vanish. Therefore,  $h$  is not considered at all during the calculation. The spherical image of  $\Phi_0$  is denoted by  $\varphi_0$ . At latitude  $\Phi_0$ ,  $k = 1$ . Using (31) for  $k$ :

$$\frac{v(\Phi_0) R n \cos \varphi_0}{c \cos \Phi_0} = 1 \quad (37)$$

That is:

$$R = \frac{c \cos \Phi_0}{v(\Phi_0) n \cos \varphi_0} \quad (38)$$

The first derivative of  $k$ :

$$\frac{dk}{d\Phi} = R n \frac{\frac{dv}{d\Phi} \cos \varphi \cos \Phi - v(\Phi) \sin \varphi \frac{d\varphi}{d\Phi} \cos \Phi + v(\Phi) \cos \varphi \sin \Phi}{c \cos^2 \Phi} \quad (39)$$

$d\varphi/d\Phi$  is given in (32) and  $dv/d\Phi$  is given in (26). This simplifies to:

$$\frac{dk}{d\Phi} = \frac{n R \cos \varphi \sin \Phi}{c v(\Phi) \cos^2 \Phi} - \frac{c \tan \varphi}{R v^3(\Phi)} \quad (40)$$

This must be zero at  $\Phi_0$ . Substituting (38) for  $R$ :

$$\frac{\tan \Phi_0}{v^2(\Phi_0)} - \frac{n \sin \varphi_0}{v^2(\Phi_0) \cos \Phi_0} = 0 \quad (41)$$

Which is solved for  $n$ :

$$n = \frac{\sin \Phi_0}{\sin \varphi_0} \quad (42)$$

To calculate  $\varphi_0$ , we need first to compute the second derivative of  $k$ . It can be done in the same way as the first derivative. However, the result is not listed here as the formula is excessively long. Nevertheless, after substituting  $\Phi = \Phi_0$ , using (38) for  $R$  and (42) for  $n$ , the second derivative gets surprisingly simple:

$$\left. \frac{d^2 k}{d\Phi^2} \right|_{\Phi=\Phi_0} = \frac{1}{v^2(\Phi_0)} - \frac{\tan^2 \Phi_0}{v^4(\Phi_0) \tan^2 \varphi_0} \quad (43)$$

As this was required previously to be zero, it follows that:

$$\tan \varphi_0 = \frac{\tan \Phi_0}{v(\Phi_0)} \quad (44)$$

Substituting (42) into (38):

$$R = \frac{c \tan \varphi_0}{v(\Phi_0) \tan \Phi_0} \quad (45)$$

So now we can use relation (44) to get the final result for  $R$ :

$$R = \frac{c}{v^2(\Phi_0)} = \sqrt{M(\Phi_0) N(\Phi_0)} \quad (46)$$

This practically means that the radius of the auxiliary sphere is the radius of the osculating sphere. It is interesting that the Gaussian conformal sphere [2] results in almost exactly the same parametrization. Given  $\Phi_0$ , (44) yields its spherical image  $\varphi_0$ . Then we can use (46) to get  $R$  and (42) to get  $n$ . The latter is undetermined if  $\Phi_0 \rightarrow 0$ . In this case,  $n \rightarrow \sqrt{1 + (e')^2}$ . Constant  $\kappa$  can be solved from (33) (this is the only formula that differs from the Gaussian sphere):

$$\kappa = \sin \varphi_0 - \frac{a^2(1 - e^2)}{R^2 n} \left( \frac{1}{2} \cdot \frac{\sin \Phi_0}{1 - e^2 \sin^2 \Phi_0} + \frac{1}{4e} \ln \frac{1 + e \sin \Phi_0}{1 - e \sin \Phi_0} \right) \quad (47)$$

It should be examined in a future paper, whether the low-distortion rectifying sphere has a similar parametrization.

## 5 Development of the double mapping

Now, we can construct an ellipsoidal oblique LAEA as a double mapping. First, we set  $\lambda_0$  of the authalic sphere to the desired longitude of origin (this makes it possible to blindly use  $\lambda_0 = 0$  during the sphere-to-plane projection). We map the latitude of origin  $\Phi_0$  to the authalic sphere to get  $\varphi_0$ . After computing these constants, we can map any point on the ellipsoid to the plane by successively applying the formulae of the authalic sphere and the spherical oblique LAEA.

The distortions of a conformal double mapping are quite easily calculated as the product of linear or areal scales of both mappings. We are not so lucky with equal-area double mappings, as calculation becomes non-trivial. The best bet is to use the general formulae of Tissot [11] (note that equal-area mappings always satisfy  $hk \sin \vartheta = 1$  simplifying the original equations):

$$h = \frac{\sqrt{\left(\frac{\partial x}{\partial \Phi}\right)^2 + \left(\frac{\partial y}{\partial \Phi}\right)^2}}{M(\Phi)} \quad (48)$$



$$k = \frac{\sqrt{\left(\frac{\partial x}{\partial \lambda}\right)^2 + \left(\frac{\partial y}{\partial \lambda}\right)^2}}{N(\Phi) \cos \Phi} \quad (49)$$

$$A + B = \sqrt{h^2 + k^2 + 2hk \sin \vartheta} \quad (50)$$

$$A - B = \sqrt{h^2 + k^2 - 2hk \sin \vartheta} \quad (51)$$

$$\omega = 2 \arcsin \frac{A - B}{A + B} = 2 \arcsin \sqrt{\frac{h^2 + k^2 - 2}{h^2 + k^2 + 2}} \quad (52)$$

Here,  $A$  and  $B$  are the maximal and minimal linear scales,  $\omega$  is the maximum angular deviation and  $\vartheta$  is the intersection angle between graticule lines (we do not need its value, as it is canceled). The partial derivatives needed for the calculations were computed manually using the chain rule. Results are listed in Appendix A.

The double mapping of Snyder [10] uses constants  $\kappa = 0$ ,  $n = 1$ , and  $R$  equal to the authalic radius. However, this authalic sphere distorts angles at the latitude of origin. This is really unwanted, as the LAEA should be distortion-free here. Snyder recognized it and corrected for it by an equal-area affine transform:

$$x' = x/m \quad (53)$$

$$y' = my \quad (54)$$

To calculate the resulting distortions, all partial derivatives of  $x$  must be multiplied by  $1/m$  and derivatives of  $y$  by  $m$ . The angular distortions are cancelled in the origin, if  $m$  is equal to linear scale  $k$  of the authalic sphere, cf. Eq. (31):

$$m = k_0 = \frac{R \cos \varphi_0}{N(\Phi_0) \cos \Phi_0} \quad (55)$$

Although this transformation does restore the desired conformality in the origin, it is kind of hacky. Furthermore, the affine transform affects the azimuthality (Snyder confirms that his version of the LAEA is slightly non-azimuthal).

A more elegant solution is proposed. We shall use the parameters of the low-distortion authalic sphere introduced in the previous section for  $n$ ,  $\kappa$ , and  $R$ . This auxiliary sphere has absolutely no distortion along its standard parallel. The derivatives of the linear scales, which determine the curvature of mapped geodesics [5], are zero here (even the second derivatives are zero). This means that azimuthality is not lost. (Strictly speaking, it is only lost to a negligible extent, as geodesics are not mapped to perfect great circles, they are ‘only’ a third-order approximation of great circles near the latitude of origin.)

The most obvious advantage of the low-distortion authalic sphere is that it contributes to the distortion pattern of the double mapping only to a completely negligible extent. To demonstrate it, the author set  $\Phi_0 = 52^\circ$ ,  $\Lambda_0 = 10^\circ$ , which are the parameters of the system LAEA-EU [3]. Then he computed maximum angular deviation  $\omega$  on a unit sphere and on ellipsoid WGS84 (the latter were computed both using Snyder’s solution and the low-distortion sphere). Python code is available as a supplementary material. Results are listed in Table 1 and Figure 1.

It is easy to see on the figure (especially along the central meridian) that while isolines of the spherical estimate and the low-distortion sphere almost coincide, Snyder’s isolines slightly deviate from them to the South. This is the result of the distortions caused by his

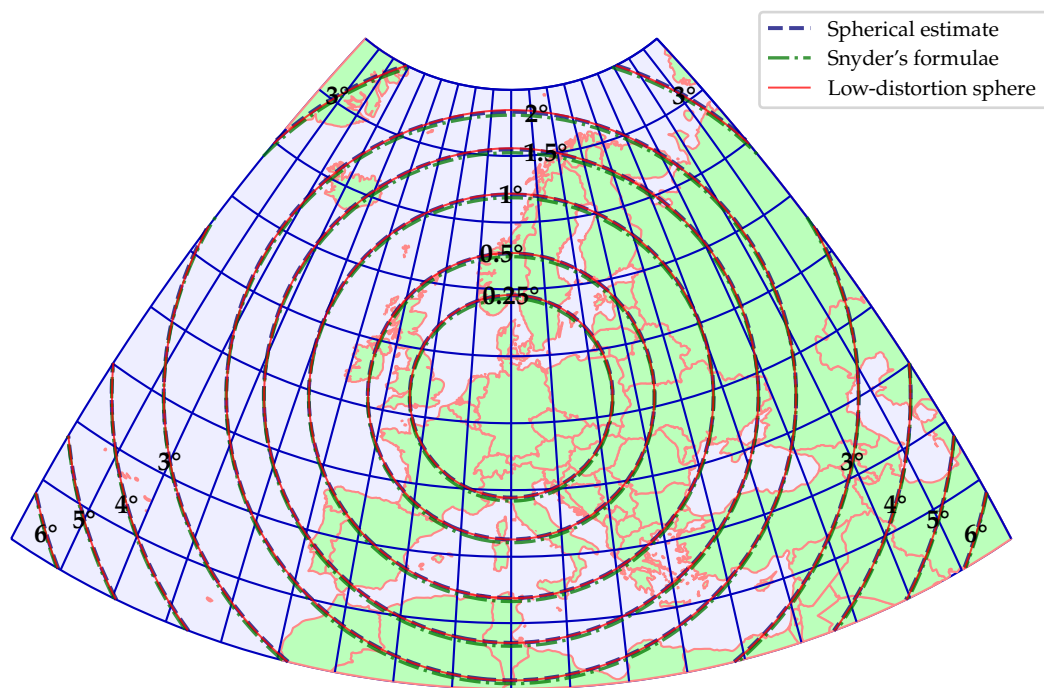


Figure 1: Comparison of angular distortions in the spherical LAEA, Snyder's double mapping and the double mapping through the low-distortion authalic sphere

$\Phi$	$\Lambda$	$\omega_{\text{Sphere}}$	$\omega_{\text{Snyder}}$	$\omega_{\text{Low-dist}}$
30	10	2.1228	2.0747	2.1248
42	10	0.4362	0.4149	0.4369
54	10	0.0174	0.0218	0.0175
66	10	0.8521	0.8884	0.8573
30	28	2.9002	2.8589	2.9058
42	28	1.0864	1.0685	1.0870
54	28	0.5286	0.5350	0.5273
66	28	1.2152	1.2483	1.2148
30	46	5.2255	5.1961	5.2334
42	46	3.0189	3.0074	3.0161
54	46	2.0383	2.0495	2.0329
66	46	2.2732	2.3057	2.2651

Table 1: Comparison of angular distortions in the spherical LAEA, Snyder’s double mapping and the double mapping through the low-distortion authalic sphere (all numbers are in degrees).

authalic sphere. The table confirms it numerically: while the angular deviations of the double mapping through the low-distortion sphere differs less than 0.1% from a spherical estimation even far from the origin, the difference of Snyder’s double mapping can exceed 1%.

This is not a merely theoretical point. As the distortions of double mappings are not calculated easily (the author found no literature listing formulae for the distortions of Snyder’s LAEA), distortions are calculated only for spherical map projections. For example, the decision-support material of the LAEA-EU [12] includes a figure for expected angular deviations. The author examined that map, and concluded that, based on the actual location of isolines, angular deviations must have been calculated for the sphere and not for the ellipsoid of revolution.

The low-distortion authalic sphere also has some disadvantages. First, as mentioned before, its inverse does not have a simple series representation. Examining its behaviour, the author found that  $\Phi \approx \varphi$  everywhere close to the standard parallel (this is where the auxiliary sphere should be used). Using this approximation as a starting value of the Newton–Raphson rule, the convergence was fast. Accuracy of  $10^{-12}$  radians were achieved in 4 iterations. For very high latitudes (ca.  $\varphi > 89.9^\circ$ ), the method does not converge with this starting value, but it converges (albeit very slowly) if the starting value is decreased by a few arcminutes.

The spherical latitude cannot be greater than  $90^\circ$ . It is a problem, if we want to use the low-distortion authalic sphere for polar regions. If  $\Phi_0 = 52^\circ$ ,  $\varphi = 90^\circ$  corresponds to  $\Phi \approx 89^\circ 30' 52''$  on WGS84. Latitudes greater than this cannot be displayed at all (results in taking the arcsine of a number greater than 1). This limiting latitude moves to the North, as  $\Phi_0$  is increased, and  $\Phi_0 = 90^\circ$  is also feasible. On the other hand, it moves to the South if  $\Phi_0$  is decreased, reaching  $\Phi \approx 87^\circ 17' 56.7''$  for  $\Phi_0 = 0^\circ$ . This should not be a practical problem as long as the pole is not displayed on the map (the double stereographic projection has similar problems very close to the poles, and it does not influence its practical usefulness).

## 6 Wrapping up

In this paper, a new realization of the oblique LAEA projection was developed. This is not a drop-in replacement of Snyder's LAEA, its planar coordinates and distortions slightly differ. Therefore, it cannot be used for existing coordinate systems, but one may consider it when defining new ones. Its major advantage is that it is closer to the spherical LAEA, one may neglect the differences between the spherical and ellipsoidal maps. While developing the formulation, the inverse formulae of the spherical LAEA were revised. The new spherical inverse equations are more stable and can be used to replace existing implementations of the spherical LAEA or the sphere-to-plane part of Snyder's double mapping.

It was a theoretically interesting result that the parametrization of the low-distortion authalic sphere closely resembles that of the Gaussian conformal sphere. The reasons of it should be investigated in the future.

## References

- [1] ADAMS, O. S. Latitude developments connected with geodesy and cartography. Tech. Rep. 67, Department of Commerce, U. S. Coast and Geodetic Survey, Washington. D.C., 1921.
- [2] GAUß, C. F. Erste Abhandlung. In *Untersuchungen über Gegenstände der Höheren Geodäsie*. Wilhelm Engelmann, Leipzig, DE, 1843, p. 3–35.
- [3] IOGP. EPSG geodetic parameter dataset. [https://epsg.org/crs\\_3035/ETRS89-extended-LAEA-Europe.html](https://epsg.org/crs_3035/ETRS89-extended-LAEA-Europe.html), 2021.
- [4] KARNEY, C. F. F. Algorithms for geodesics. *Journal of Geodesy* 87, 1 (2013), 43–55. doi:10.1007/s00190-012-0578-z.
- [5] KERKOVITS K. Calculation and visualization of flexion and skewness. *Kartografija i geoinformacije* 17, 29 (2018), 32–45.
- [6] KESSLER, F., AND BATTERSBY, S. *Working with Map Projections: A Guide to their Selection*, 1 ed. CRC Press, Boca Raton, FL, 2019. doi:10.1201/9780203731413.
- [7] LAPAINE, M., AND FRANČULA, N. Map projection aspects. *International Journal of Cartography* 2, 1 (2016), 38–58. doi:10.1080/23729333.2016.1184554.
- [8] PANASIUK, J., GDOWSKI, B., AND BALCERZAK, J. The Roussilhe projection of the entire ellipsoid. In *Proc. of the 16th International Cartographic Conference* (Cologne, DE, 1993), P. Mesenburg, Ed., vol. 2, p. 1277–1286.
- [9] ŠAVRIČ, B., JENNY, B., AND JENNY, H. Projection wizard – an online map projection selection tool. *The Cartographic Journal* 53, 2 (2016), 177–185. doi:10.1080/00087041.2015.1131938.
- [10] SNYDER, J. P. *Map projections: A working manual*. No. 1395. U.S. Government Printing Office, Washington, D.C., 1987. doi:10.3133/pp1395.
- [11] TISSOT, N. A. *Mémoire sur la représentation des surfaces et les projections des cartes géographiques*. Gauthiers-Villars, Paris, 1881.

- [12] TSOULOS, L. An equal area projection for statistical mapping in the EU. In *Map Projections for Europe*, A. Annoni, C. Luzet, E. Gubler, and J. Ihde, Eds. Institute for Environment and Sustainability, 2001, p. 50–55.
- [13] VAN HEES, S. *Globale en lokale geodetische systemen*, 4 ed. Nederlandse Commissie voor Geodesie, Delft, NL, 2006. isbn:9789061322948.
- [14] WRAY, T. The seven aspects of a general map projection. *Cartographica* 11, 2 (1974), 1–72. doi:10.3138/E382-8522-4783-28K5.

## A Calculating the derivatives of the double mapping

$$\begin{aligned}
 \frac{d\varphi}{d\Phi} &= \frac{M(\Phi) N(\Phi) \cos \Phi}{R^2 n \cos \varphi} \\
 \frac{d\lambda}{d\Lambda} &= n \\
 \frac{\partial \varphi'}{\partial \varphi} &= \frac{\cos \varphi \sin \varphi_0 - \sin \varphi \cos \varphi_0 \cos \lambda}{\cos \varphi'} \\
 \frac{\partial \varphi'}{\partial \lambda} &= \frac{-\cos \varphi \cos \varphi_0 \sin \lambda}{\cos \varphi'} \\
 \frac{\partial \lambda'}{\partial \varphi} &= \frac{-\sin \lambda \sin \varphi \cos \lambda' + (\sin \varphi \sin \varphi_0 \cos \lambda + \cos \varphi \cos \varphi_0) \sin \lambda'}{\cos \varphi'} \\
 \frac{\partial \lambda'}{\partial \lambda} &= \frac{\cos \lambda \cos \varphi \cos \lambda' + \cos \varphi \sin \varphi_0 \sin \lambda \sin \lambda'}{\cos \varphi'} \\
 \frac{\partial x}{\partial \varphi'} &= \frac{-R \sin \lambda' \cos \varphi'}{\sqrt{2} \sqrt{1 - \sin \varphi'}} \\
 \frac{\partial x}{\partial \lambda'} &= \frac{\sqrt{2} R \cos \lambda' \cos \varphi'}{\sqrt{1 + \sin \varphi'}} \\
 \frac{\partial y}{\partial \varphi'} &= \frac{R \cos \lambda' \cos \varphi'}{\sqrt{2} \sqrt{1 - \sin \varphi'}} \\
 \frac{\partial y}{\partial \lambda'} &= \frac{\sqrt{2} R \sin \lambda' \cos \varphi'}{\sqrt{1 + \sin \varphi'}} \\
 \frac{\partial x}{\partial \Phi} &= \left( \frac{\partial x}{\partial \varphi'} \frac{\partial \varphi'}{\partial \varphi} + \frac{\partial x}{\partial \lambda'} \frac{\partial \lambda'}{\partial \varphi} \right) \frac{d\varphi}{d\Phi} \\
 \frac{\partial x}{\partial \Lambda} &= \left( \frac{\partial x}{\partial \varphi'} \frac{\partial \varphi'}{\partial \lambda} + \frac{\partial x}{\partial \lambda'} \frac{\partial \lambda'}{\partial \lambda} \right) \frac{d\lambda}{d\Lambda} \\
 \frac{\partial y}{\partial \Phi} &= \left( \frac{\partial y}{\partial \varphi'} \frac{\partial \varphi'}{\partial \varphi} + \frac{\partial y}{\partial \lambda'} \frac{\partial \lambda'}{\partial \varphi} \right) \frac{d\varphi}{d\Phi} \\
 \frac{\partial y}{\partial \Lambda} &= \left( \frac{\partial y}{\partial \varphi'} \frac{\partial \varphi'}{\partial \lambda} + \frac{\partial y}{\partial \lambda'} \frac{\partial \lambda'}{\partial \lambda} \right) \frac{d\lambda}{d\Lambda}
 \end{aligned}$$